The Impact of Changes in InFeed Rate on Surface Integrity after Chrome Plate Grinding by Microcrystalline Corundum

Martin Marek, Martin Novák, Karel Šramhauser
Faculty of Mechanical Engineering, J. E. Purkyně University in Usti nad Labem, Pasteurova 3334/7, 400 01 Ústí nad Labem. Email: martin.marek@ujep.cz, martin.novak1@ujep.cz, karel.sramhauser@ujep.cz

The efficient processing of materials, the development of machine concepts and grinding tools, as well as growing environmental and economic pressure are existing challenges in grinding. Chromium coatings are mainly used for components where corrosion protection is required, but also for the repair of worn parts. This paper presents and discusses the possibilities of utilizing changes in feed rate to achieve guaranteed surface integrity, which is very important for the life of the component. The results are presented in the form of tables and graphs, where I focus mainly on parameters of surface roughness and circularity.

Keywords: grinding, surface integrity, cutting conditions, hard chrome coating

1 Introduction

Grinding is an abrasive cutting process for producing accurate dimensions and cuts on various materials. This process is one of the most used for finishing operations, but also can help in mass production that requires removing large amounts of roughed out material. Grinding is a characteristic process that is influenced by several factors: large cutting forces, the generation of a large amount of heat due to irregularities of the grinding wheel, irregular chip removal, irregular geometry of the cutting edge, a small cross-section of the chip, self-sharpening of the grinding wheel, high cut rates (typically 35 m.s^{-1}, sometimes above 100 m.s^{-1}), residual stresses, the amount of deformation in the areas of primary and secondary deformation, and in the area of contact of the tool with the machined surface, cutting environment and more.[1-6]

In a wide range, surface integrity can be separated into two aspects: the internal subsurface layers of microstructure, mechanical properties and residual stresses and of external topography of surfaces (surface finish). Experts in the field around the world have gathered together research on surface integrity after grinding. Topics enclosed include: surface topography evaluation and characterization, the definition of surface integrity, the mechanical properties of subsurface layers and microstructure modification, residual stresses, surface integrity aspects in machining processes and surface integrity characterization methods, etc. [7-10]

Hard chrome plating is a significant surface treatment of nominated mechanical components, which significantly increases the life of individual parts. The quality of chrome plating depends on the selection of the right technological process. Chromium coatings are mainly used for components where corrosion protection is required. In this case, the chrome coating is applied due to increased surface hardness, abrasion resistance and high temperature resistance. For this experiment, the chromium process was chosen because of its widespread use in refurbishing parts after dismantling gas turbines and subsequently assembling them. [11-16]

The aim of this research was to find optimal cutting conditions when grinding wheels based on microcrystalline corundum were used, where the main consideration in measurement and evaluation was circularity and roughness of the surface and its profile after grinding. This experiment was in cooperation with Solar Turbines EAME L.t.d.

2 Plan of experiment and cutting conditions

The aim of this experiment was grinding chrome platied rings (Fig. 1).
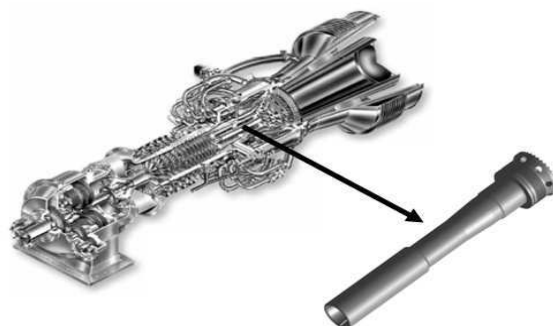

***Fig. 1** Example of pattern*

***Fig. 2** A sample of the shaft from the combustion part of the turbine which has been cut*

These rings were cut at the frame saw mill. The next operation for preparation of samples was machining the

heads of samples and the drilled inner diameter. The last operation was galvanic plating with chromium, where the thickness was around 0.4 mm. The base material was chrome-nickel-molybdate steel (shaft – Fig. 2), which corresponds with AMS 6415.

In Tab. 1 it is possible to see the chemical composition of the base material, which was analysed by Q4 TASMAN optical emission spectrometer (Fig. 3). All values are supplemented by a standard deviation.

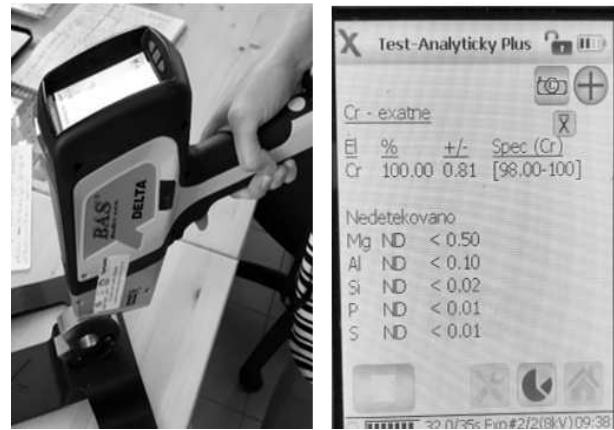**Fig. 3** *Q4 TASMAN optical emission spectrometer*

Fig. 4 *DELTA optical spectrometry and chemical composition of chromium layer*

For verification of the galvanic chromium layer, the analysis was carried out using the DELTA Handheld Optical Spectrometer (Fig. 4). It can be seen from the figure that the chemical composition of the galvanized layer is almost 100 % chromium.

Hakufluid 182 procedural fluid was used for the experiment. This process liquid is water-based with a 4 - 7 % concentration and was chosen based on previous experiments. For grinding, the AG 92/99 150J 9V grinding tool was chosen, which is characterized by high hardness, porous structure, moderate grain size and a ceramic binder. The grains of the grinding wheel show a higher material removal rate and a lower number of dressing cycles. The selected grinding wheel has a maximum permissible circumferential velocity of 40 m.s-1. A 0.1 mm depth removal rate was chosen. All cutting conditions are shown in Tab. 2.

Tab. 1 *Chemical composition*

	Chemical composition of base material [hm. %]								
Element	**C**	**Mn**	**P**	**Cr**	**Mo**	**S**	**Ni**	**Si**	**Fe**
%	0.415	0.711	< 0.005	0.817	0.234	< 0.001	1.835	0.263	95.300
±σ	0.004	0.004	-	0.003	0.001	-	0.008	0.003	0.010

Tab. 2 *Cutting condition*

Material	Grinding wheel	Cutting conditions			No. sample
		Vw	**Vc**	**Vf**	
Galvanic Chrome plate	AG 92/99 150J 9V	15 m.min-1	30 m.s-1	0.13 mm.min-1	A1
				0.17 mm.min-1	A2
				0.26 mm.min-1	A3
				0.41 mm.min-1	A4
				0.64 mm.min-1	A5
			40 m.s-1	0.13 mm.min-1	A6
				0.17 mm.min-1	A7
				0.26 mm.min-1	A8
				0.41 mm.min-1	A9
				0.64 mm.min-1	A10

The surface roughness and its profile were measured using the T8000 Hommel Tester. which measures the surface according to the CSN EN ISO 4287 standard. Each sample was measured 12x at 30 ° to obtain values along the entire circumference. For surface roughness I worked with parameters such as Ra. Rz. Rt. Rq. Rmax. Rpk and Rvk. I was also dealing with characteristics of the material and surface profile. From all 12 values for each sample the arithmetic mean was calculated and supplemented by a standard deviation. Surface roughness values are shown in Table 3.

Tab. 3 *Average values of surface roughness*

No sample		Ra [µm]	Rz [µm]	Rt [µm]	Rmax [µm]	Rpk [µm]	Rvk [µm]	Rq [µm]
A1_1	Arithmetic Average	0.194	1.418	1.730	1.664	0.213	0.335	0.245
	Standart Deviation	0.007	0.061	0.138	0.163	0.024	0.026	0.009
A1_2	Arithmetic Average	0.176	1.287	1.618	1.537	0.198	0.267	0.22
	Standart Deviation	0.011	0.085	0.248	0.231	0.018	0.02	0.013
A2_1	Arithmetic Average	0.236	1.657	2.077	2.037	0.271	0.346	0.296
	Standart Deviation	0.01	0.096	0.209	0.173	0.029	0.028	0.013
A2_2	Arithmetic Average	0.238	1.603	1.963	1.920	0.258	0.313	0.295
	Standart Deviation	0.007	0.071	0.198	0.229	0.023	0.046	0.008
A3_1	Arithmetic Average	0.258	1.791	2.273	2.138	0.275	0.378	0.323
	Standart Deviation	0.006	0.056	0.182	0.140	0.048	0.033	0.008
A3_2	Arithmetic Average	0.274	1.939	2.363	2.218	0.339	0.371	0.344
	Standart Deviation	0.007	0.116	0.231	0.169	0.018	0.025	0.008
A4_1	Arithmetic Average	0.297	2.050	2.50	2.382	0.334	0.427	0.373
	Standart Deviation	0.011	0.165	0.351	0.215	0.046	0.056	0.016
A4_2	Arithmetic Average	0.297	2.187	2.641	2.503	0.363	0.486	0.378
	Standart Deviation	0.01	0.125	0.262	0.229	0.051	0.052	0.015
A5_1	Arithmetic Average	0.337	2.392	2.943	2.825	0.401	0.519	0.424
	Standart Deviation	0.015	0.132	0.225	0.169	0.031	0.045	0.017
A5_2	Arithmetic Average	0.331	2.368	2.864	2.731	0.400	0.506	0.417
	Standart Deviation	0.010	0.135	0.244	0.206	0.043	0.062	0.014
A6_1	Arithmetic Average	0.271	1.811	2.152	2.077	0.262	0.417	0.336
	Standart Deviation	0.009	0.086	0.23	0.173	0.026	0.046	0.011
A6_2	Arithmetic Average	0.268	1.952	2.387	2.297	0.307	0.44	0.339
	Standart Deviation	0.015	0.183	0.259	0.231	0.031	0.073	0.02
A7_1	Arithmetic Average	0.292	2.021	2.435	2.297	0.341	0.379	0.365
	Standart Deviation	0.008	0.124	0.306	0.320	0.039	0.045	0.012
A7_2	Arithmetic Average	0.298	2.075	2.486	2.395	0.322	0.543	0.377
	Standart Deviation	0.008	0.092	0.163	0.144	0.02	0.052	0.009
A8_1	Arithmetic Average	0.301	1.986	2.354	2.255	0.321	0.487	0.377
	Standart Deviation	0.011	0.09	0.127	0.157	0.034	0.076	0.013
A8_2	Arithmetic Average	0.304	2.143	2.584	2.505	0.376	0.432	0.383
	Standart Deviation	0.006	0.08	0.235	0.223	0.042	0.025	0.007
A9_1	Arithmetic Average	0.323	2.167	2.598	2.475	0.289	0.524	0.402
	Standart Deviation	0.008	0.115	0.227	0.166	0.032	0.061	0.009
A9_2	Arithmetic Average	0.315	2.401	3.099	2.92	0.384	0.555	0.402
	Standart Deviation	0.020	0.130	0.292	0.296	0.054	0.079	0.027
A10_1	Arithmetic Average	0.361	2.517	2.997	2.877	0.443	0.533	0.453
	Standart Deviation	0.011	0.127	0.19	0.235	0.035	0.051	0.014
A10_2	Arithmetic Average	0.363	2.481	3.14	3.079	0.385	0.552	0.454
	Standart Deviation	0.015	0.148	0.365	0.400	0.043	0.105	0.019

Circularity measurements were performed on the T4004 Hommel Tester Form according to CSN EN ISO 4298. The circularity indicator is often used in practice for the examination of precisely machined circular parts where the desired tolerance is compared. Measurement was done 3 times. Once in the middle and on each edge of the sample. From the measured values I calculated the arithmetic mean and the standard deviation. Circular values are in Table 4.

***Tab. 4** Average values of circularity*

	A1_1	A2_1	A3_1	A4_1	A5_1	A6_1	A7_1	A8_1	A9_1	A10_1
Arithmetic Average	1.263	4.073	4.970	6.243	3.700	2.903	3.517	3.367	2.313	3.633
Standart Deviation	0.355	0.240	0.569	0.380	0.104	0.551	0.125	0.447	0.228	0.242
	A1_2	A2_2	A3_2	A4_2	A5_2	A6_2	A7_2	A8_2	A9_2	A10_2
Arithmetic Average	0.750	3.333	4.760	4.580	4.673	6.183	3.887	1.703	4.030	2.123
Standart Deviation	0.075	0.254	0.337	0.216	0.667	0.680	0.055	0.357	0.525	0.429

3 Evaluation of surface roughness

The next series of graphs have yellow bars to show cutting speed for the grinding wheel from 30 m.s^{-1} and grey bars show cutting speed for the grinding wheel from 40 m.s^{-1}. A light color is used for the first measurement and a dark color is used for verification of the grinding on new samples.

3.1 Average arithmetic deviation analysis – Ra and Rz

In the following fig. 5 roughness Ra depends on the infeed rate. The lowest value Ra 0.194 ± 0.007 µm was achieved with an infeed rate of 0.13 mm.min^{-1} and cutting speed of 30 m.s^{-1}. During the verification process, a value of Ra 0.176 ± 0.011 µm was achieved. By adding the standard deviation to the first grinding and subtracting the standard deviation for the second grinding, the values are within their range. The highest value Ra 0.337 ± 0.015 µm was achieved with an infeed rate of 0.64 mm.min^{-1} and cutting speed of 30 mm.s^{-1}. Verification using these settings resulted in a value of Ra 0.331 ± 0.010 µm. By

subtracting the standard deviation for the first grinding and adding for the second grinding, the values are within their range. Looking at table 3, it can be seen that values with a cutting speed of 40 m.s^{-1} were increased about 5 – 20 %. The biggest change or increase occurred at a feed rate of 0.17 mm.min^{-1}.

Fig 6. shows the dependence of surface rougness Rz on infeed rate. This parameter Rz has very similar dependence as parameter Ra. The parameter Rz shows the maximum and minuimum height of the protrusion in the measured length lr. The lowest value was achieved for sample no. A1, where an infeed rate of 0.13 mm.min^{-1} and cutting speed of 30 mm.s^{-1} were used. The result was Rz 1.418 ± 0.061 µm. For cutting speed 30 mm.s^{-1} an increasing infeed rate is seen, with values increasing about 0.140 – 0.250 µm for each increase of infeed rate. Using a cutting speed of 40 mm.s^{-1} the same rise in values is seen, with the difference that the values were 5 -10 % larger with the comparison of the reduced cutting speed of 30 mm.s^{-1}. The biggest change is seen with a cutting speed of 40 mm.s^{-1} and infeed rate of 0.41 mm.min^{-1}, where value increased more than 0.4 µm.

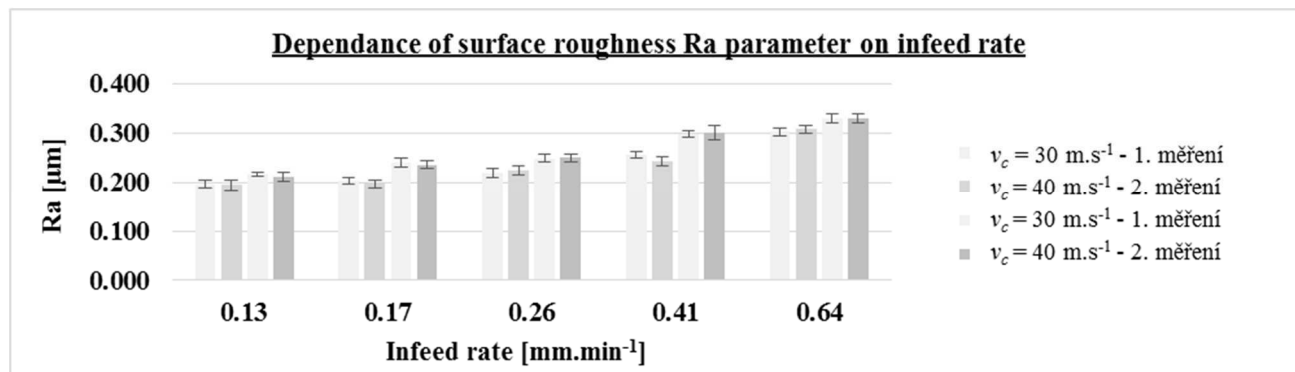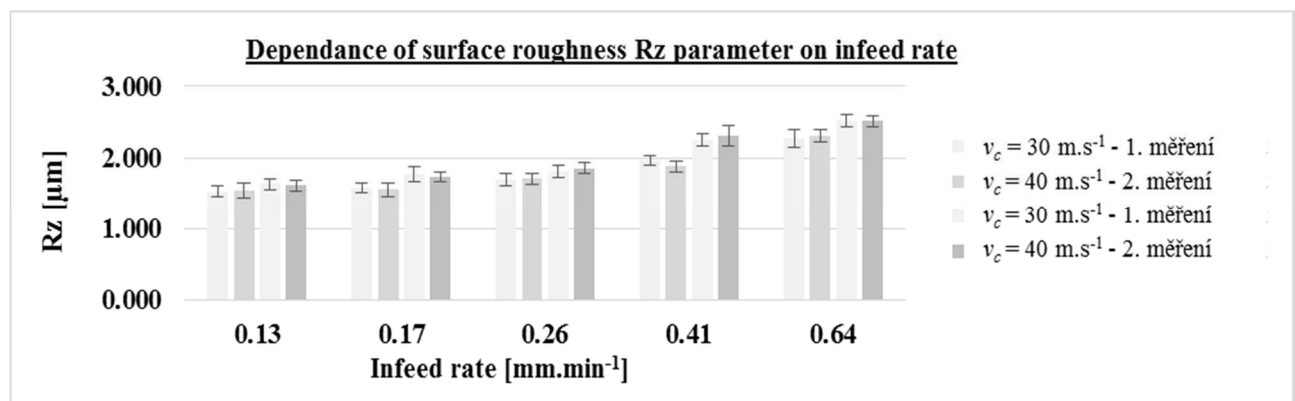***Fig. 5** The average value Ra*

***Fig. 6** The average value Rz*

3.2 Average arithmetic deviation analysis – Rt

The parameter Rt is very similar to Rz, also the sum of Rp and Rv, the difference lies in the evaluated length ln. Fig. 7 shows the relationship between infeed rate and results of Rt. Increasing the infeed rate of the grinding wheel as in the previous measurements, where the values are also increasing. The highest and lowest values are the same as in the previous graphs in Figures 5 and 6. Here, when determining the standard deviations, it can be seen that the verification grinding No. 2 is within the range of the first grinding values. Also, the magnitude of the standard deviations is at very low levels, and up to 15%.
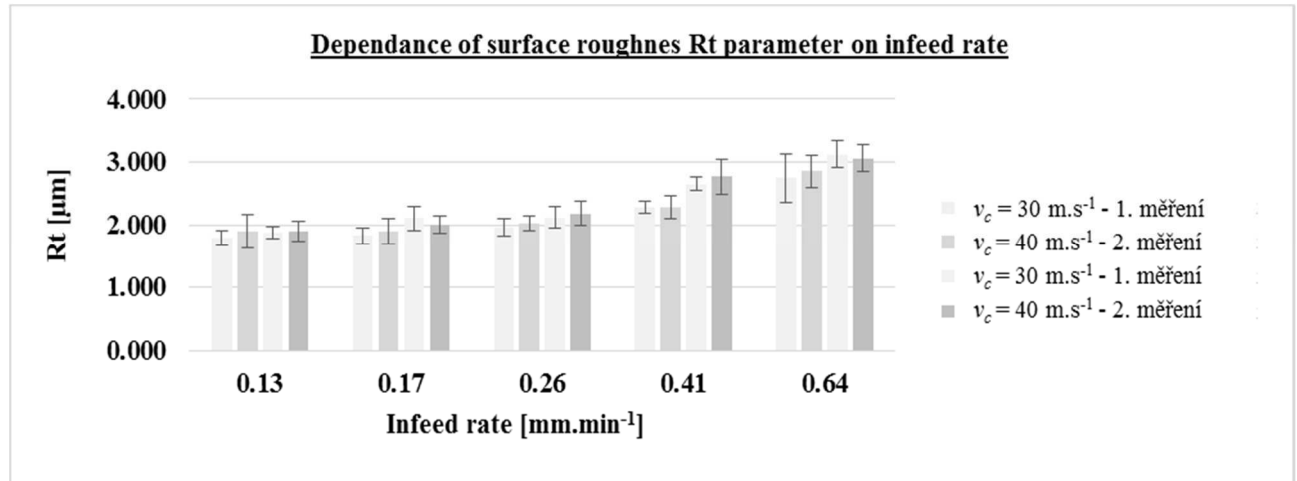

Fig. 7 The average value Rt

3.3 Average arithmetic deviation analysis – Rmax

Another parameter to be studied is Rmax. This parameter Rmax is the sum of the maximum depth value and the highest peak in the range of five fundamental lengths. The values of parameter Rz are at the same rate for infeed rates of 0.13; 0.17; 0.26 mm.min^{-1} and cutting speeds of 30 and 40 m.s^{-1}. A more pronounced increase was at a cutting speed of 40 m.s^{-1} with an infeed rate of 0.41 mm.min^{-1} and a cutting speed of 30 and 40 m.s^{-1} with an infeed rate of 0.64 mm.min^{-1}.
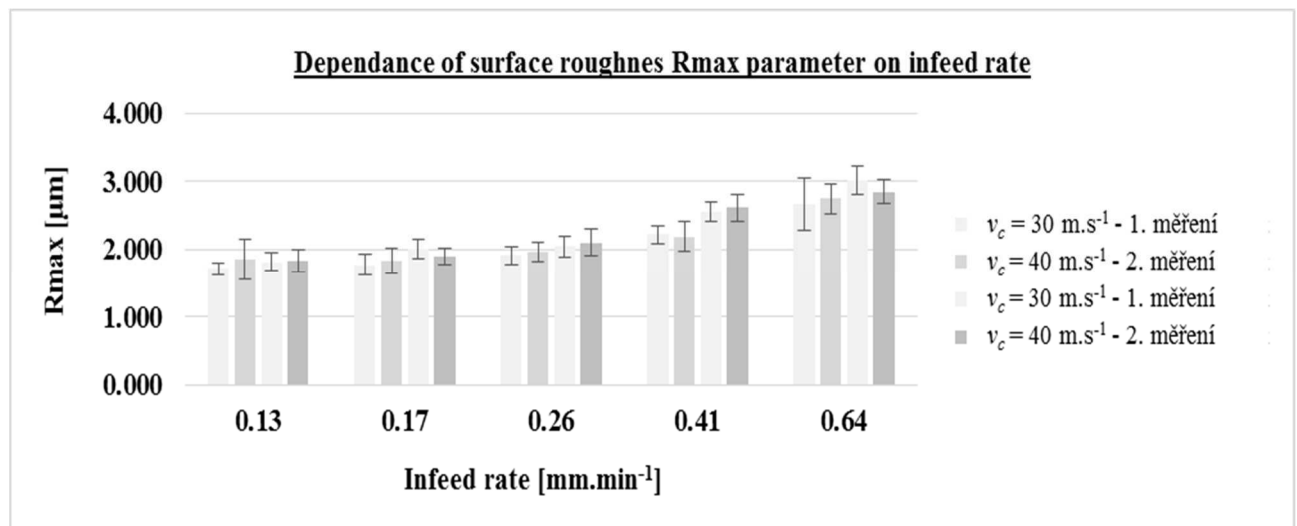

Fig. 8 The average value Rmax

3.4 Average arithmetic deviation analysis – Rpk and Rvk

Analysis of material ration curve shows a substantial influence on the functional characteristics of the component, where the size and quantity of peaks and valleys can be seen, because sometimes it is a good idea to have some peaks in the material and sometimes valleys. It depends on where components are used. Table 3 shows values for valleys and peaks. All A1 - A10 samples have larger valleys than peaks in their profile. The valleys are approximately 15 – 25 % larger than the peaks. Lower values were achieved at lower infeed rates. At a cutting speed of 40 m.s^{-1} and feed rates of 0.13 mm.min^{-1} and 0.26 mm.min^{-1}, the Rvk parameter values are lower than at a cutting speed of 30 m.s^{-1} by approximately 5 – 10 %.
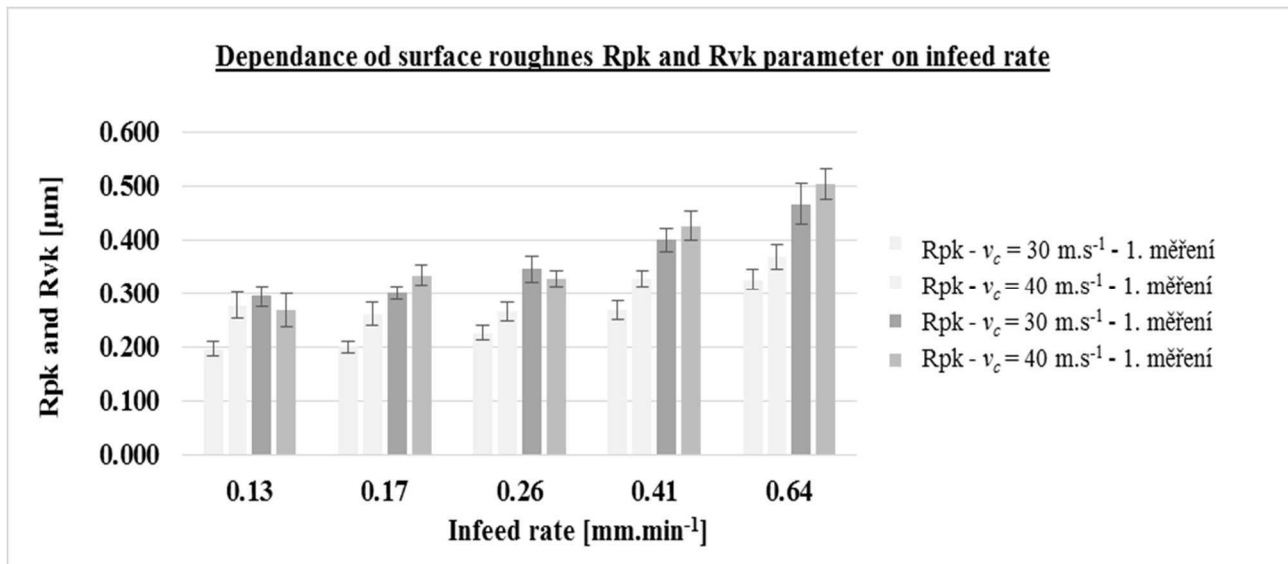
Fig. 9 *The average value Rpk and Rvk*

3.5 Analysis of surface profile

The material share curve (Abbott Firestone curve) is another integral parameter that characterizes the surface and is particularly important for dynamically loaded components. The basic purpose of the curve is the assessment of stressed functional surfaces and the solution of friction and lubrication issues. Its shape will vary depending on the surface quality. The more the curve takes the plane character, the more we can assume that the surface will exhibit lower roughness parameters. Figure 10 shows the material portions for a cutting speed of 30 m.s^{-1} and 3 different infeed rates. All three surface topologies of infeed rates 0.13; 0.26; 0.64 mm.min^{-1} are the same, only the size of the values are different. This curve shape shows a large fill of material with occasional longer recesses. In Fig. 11, for a cutting speed of 40 m.s^{-1} and the some infeed rates, the curve position was reduced. This has the significant percentage compensation represented in the material.
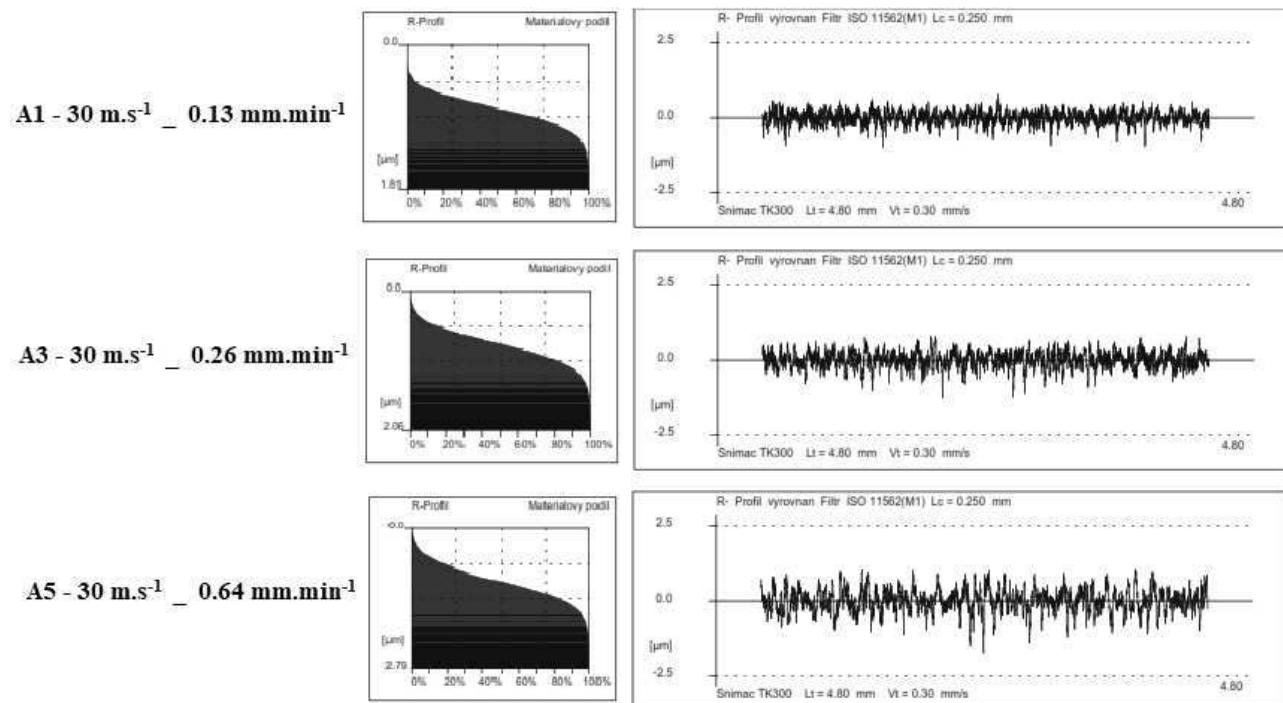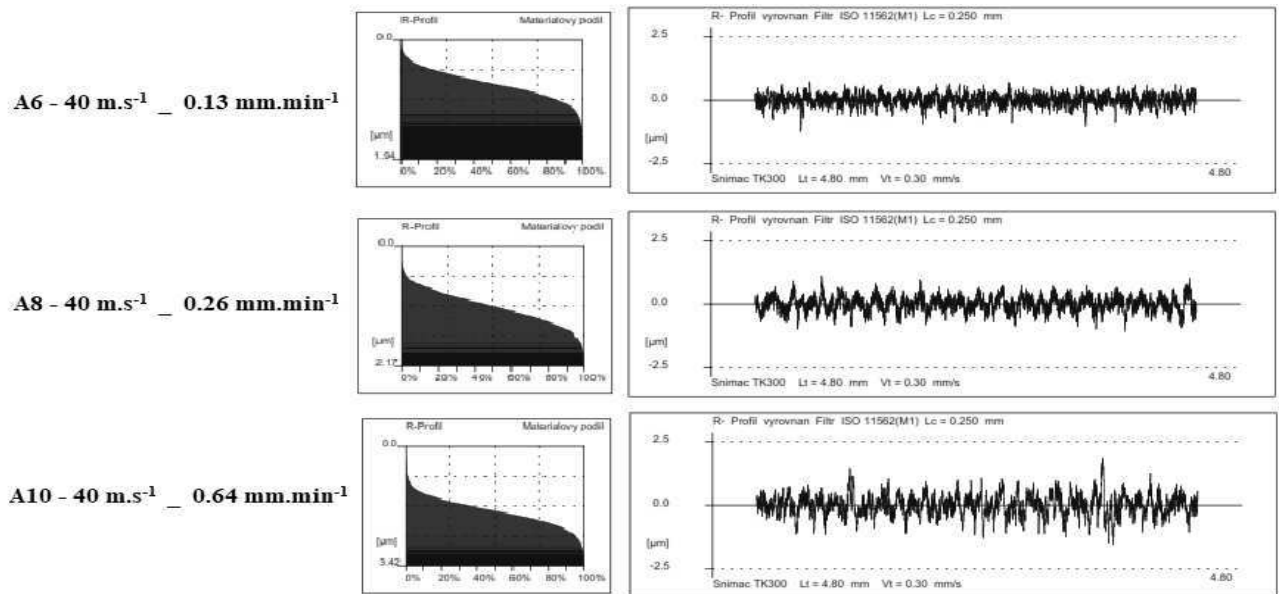

Fig. 10 *The surface profile 30 m.s^{-1}*

Fig. 11 *The surface profile 40 m.s⁻¹*

3.6 Analysis of circularity

The circularity of two cutting speeds and five infeed rates is shown on figure 12. All values were supplemented by standard deviations. The curve is not the same as the roughness of the surface. For each cutting speed and feed rate, two samples were used, so two measurements were used to compare the measured results. For a cutting speed of 30 m.s⁻¹, the lowest E value was 1.263 ± 0.355 μm at a feed rate of 0.13 mm.min⁻¹. By increasing the infeed velocity, the circularity values increased to the last infeed rate of 0.64 mm.min⁻¹, where the value slightly decreased. The highest circularity E of 6.243 ± 0.380 μm was measured at a feed rate of 0.42 mm.min⁻¹. The second measurement verified 80% of the first measurement. For a 40m.s⁻¹ cutting speed, the resulting values are unsatisfactory, because one measurement is very different from the test series. For example, at the lowest infeed rate of 0.13 mm.min⁻¹, the values changed by almost 100%. Overall, all measured results have a larger range of standard deviations. This phenomenon of divergent values could result, for example, in insufficient sample clamping, insufficient balancing, or oscillation of the SNOP system.
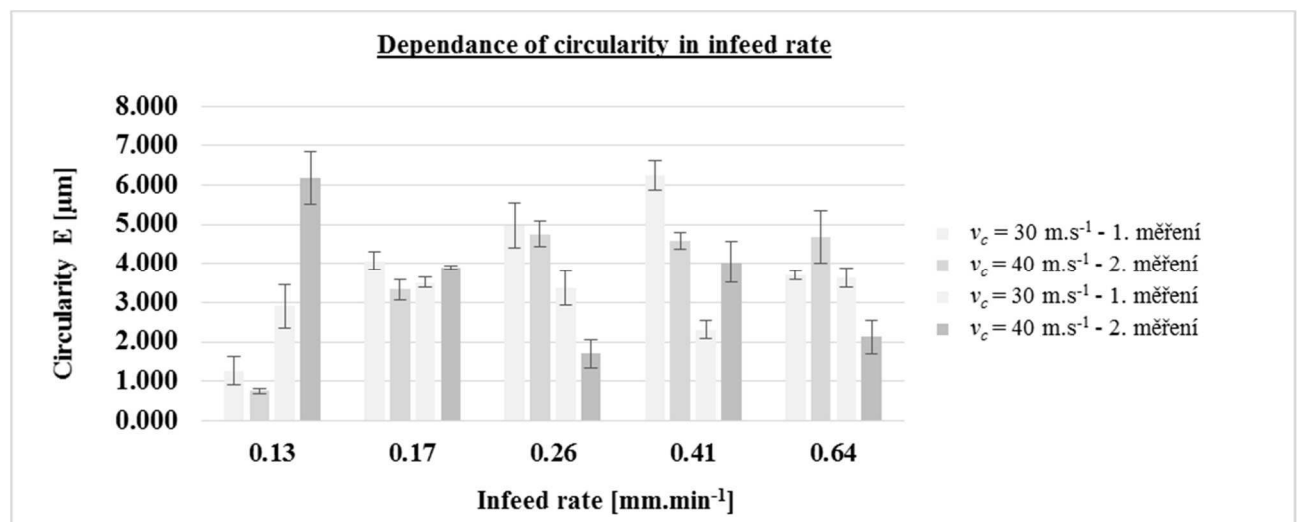

Fig. 12 *Dependance of circularity*

4 Summary

This experiment offers an explanation of changing cutting conditions on surface integrity after chrome plate grinding by microcrystalline corundum. For this experiment a total of 20 samples were tested, where 10 samples were used for the first measurement and the second 10 samples for the verification process. Cutting conditions were set to indicate the dependence of changing the cutting conditions on surface roughness and circularity. Extensive analysis of roughness parameters was due to the qualitatively rated new supplier for chrome plating and the use of new cutting conditions at grinding. The lowest values of surface rougness of Ra paramter for cutting speed of 30 m.s⁻¹ were achieved with an infeed

rate of 0.13 mm.min^{-1}, where the value of surface roughness was Ra 0.194 ± 0.007 μm. With a cutting speed of 40 m.s-1 and infeed rate 0.13 m.min^{-1}, a surface roughness of Ra 0.268 ± 0.015 μm was achieved. The highest values were achieved with cutting speeds of 30; 40 m.s^{-1} and infeed rate of 0.64 mm.min^{-1}, where the values were Ra 0.424 ± 0.017 μm and Ra 0.453 ± 0.014 μm. All measured parameters as Rz, Rt, Rmax and Rq have the same dependence as Ra, with increased infeed rates, surface roughness values were increased. During analysis of surface profiles it was seen that for all samples A1 - A10 there were larger valleys than peaks in their profile. The valleys were approximately 15 – 25 % larger than the peaks. Lower values were achieved at lower infeed rates. By focusing on circularity, it can be seen that results have almost no dependence, because the values have diferent sizes and standard deviations are also of higher dimensions.

Acknowledgement

References

[1] MÁDL. J.. KAFKA. J.. VRABEC. M.. DVOŘÁK. R. (2000). *Technologie obrábění.* 3. díl. Praha: ČVUT. 2000. 81 s.

[2] G. E. DIETER. (1989). *Mechanical Metallurgy.* McGraw Hill Higher Education. 1989.

[3] L. JIANG. J. PARO. H. HÄNNINEN. V. KAUPPINEN AND R. ORASKARI. (1996). Comparison of grindability of HIP austenitic 316L. duplex 2205 and Super duplex 2507 and as-cast 304 stainless steels using alumina wheels. *Journal of Materials Processing Technology.* vol. 62. pp. 1- 9. 1996.

[4] MAREK, M., NOVÁK, M. (2017). The Effect of Changes in Feed Rate on Surface Integrity during Nickel Coating Grinding, Solid State Phenomena, Vol. 261, pp. 207-214, 2017

[5] NOVAK, M., NAPRSTKOVA, N. (2015). Grinding of the Alloy INCONEL 718 and Final oughness of the Surface and Material Share. *In: Manufacturing Technology*, Vol. 15, No. 6 (2015) pp 1015-1023, ISSN: 1213-2489.

[6] MAREK. M.. NOVÁK. M. (2016). Hodnocení drsnosti povrchu po broušení niklového povlaku při změně řezných podmínek. *Strojírenská Technologie.* 2016. ročník XXI. číslo 1. s. 33-38. ISSN 1211 – 4162

[7] MARINESCU. Z.. D.. aj. (2007). *Handbook of machining with grinding wheels.* Boca Raton : CRC Press.2007. 592 s. ISBN 1-57444-671-1

[8] M.R KALANTARY. K.A HOLBROOK. P.B WELLS. (1993). Trans. Instut. *Metal Finishing.* 71 (2) (1993). p. 55

[9] MAREK, M., NOVÁK, M., HOLESOVSKY, F., DURAKBASA, M., N. (2017). The Effect of Changes to Nickel Coating Machine on Surface Integrity and Microstructure after Grinding, *In: Manufacturing Technology*, Vol. 17, No. 6 (2017) pp 906-912, ISSN: 1213-2489.

[10] M. FIELD AND J. KAHLES. (1964). The surface integrity of machined and ground high strength steels. pp. 210: 54-77. 1964.

[11] MAREK. M.. NOVÁK. M. (2017). The Effect of Changes in Feed Rate on Surface Integrity during Nickel Coating Grinding. *Solid State Phenomena.* Vol. 261. pp. 207-214. 2017

[12] MADL. J. (2001). Theoretival aspect of precise machining. In I. *International Congress of precision machining.* Ústí nad labem. Czech Republic : ÚTŘV. J. E. Purkyne University. 2001. s 65-69. ISBN 80-7044-358-8

[13] MAREK. M.. NOVÁK. M.. RYTINA. T.. DURAKBASA. M.. N. (2017). Process and Equipment Improvement for Nickel Brush Plating Application. In*: Manufacturing Technology*. Vol. 17. No. 4 (2017) pp 503-507. ISSN: 1213-2489

[14] Tvrdé chromování. BOMEX CZ. Bomex [online]. 1999 [cit. 2012-04-18]. Dostupné z: http://www.bomex.cz/cz/3-technologie/8-tvrde-chromovani.html

[15] JINFENG ZHANG, CHAO FENG, YUNHUI MA, WEI TANG, SHUAI WANG, XIN ZHONG. (2017). Nondestructive analysis of surface integrity in turning and grinding operations *In: Manufacturing Technology*, Vol. 17, No. 3, pp. 412-418, ISSN:1213-2489.

[16] MALLORY. G. O. a J. B. HAJDU. (1990). Electroplaters and Surface Finishers Society. *Electroless plating: fundamentals and applications*, Society, Orlando, Fla. 1990. 539pp. ISBN 978-0815512776